The Effects of Sliding Velocity on the Frictional and Physical Properties of Heated Fault Gouge

D. E. MOORE,[1] R. SUMMERS[1] and J. D. BYERLEE [1]

Abstract—The frictional properties of a crushed granite gouge and of gouges rich in montmorillonite, illite, and serpentine minerals have been investigated at temperatures as high as 600 °C, confining pressures as high as 2.5 kbar, a pore pressure of 30 bar, and sliding velocities of 4.8 and 4.8×10^{-2} μm/sec. The gouges showed nearly identical strength behaviors at the two sliding velocities; all four gouges, however, showed a greater tendency to stick-slip movement and somewhat higher stress drops in the experiments at 4.8×10^{-2} μm/sec. Varying the sliding velocity also had an effect on the mineral assemblages and deformation textures developed in the heated gouges. The principal mineralogical difference was that at 400 °C and 1 kbar confining pressure a serpentine breakdown reaction occurred in the experiments at 4.8×10^{-2} μm/sec but not in those at 4.8 μm/sec. The textures developed in the gouge layers were in part functions of the gouge type and the temperature, but changes in the sliding velocity affected, among other features, the degree of mineral deformation and the orientation of some fractures.

Key words: Fault gouge, friction, deformation textures.

Introduction

Earthquakes are generated to depths of about 20 km on transform faults such as the San Andreas (BRACE and BYERLEE, 1970), and many of the largest earthquakes are concentrated at the base of this seismogenic zone (SIBSON, 1982). To help determine the controls on stable and unstable slip along faults at such depths, friction studies at elevated temperatures need to be conducted on appropriate rock materials. The sliding characteristics of a variety of faulted rocks have been investigated at elevated temperatures and pressures (BRACE and BYERLEE, 1970; OLSSON, 1974; ENGELDER et al., 1975; STESKY et al., 1974; STESKY, 1978). Thus far, however, few such studies of heated gouge materials have been conducted (LOGAN et al., 1979, 1981; MOORE et al., 1983).

We have begun a systematic investigation of the high-temperature friction strengths of a group of four gouges. An initial set of experiments, in which the temperature and confining pressure were varied at a constant pore pressure and sliding velocity, was described in MOORE et al. (1983). This study considers the effects

[1] U.S. Geological Survey, 345 Middlefield Road, MS/977, Menlo Park, CA 94025.

Table 1

Mineralogy of Gouges Used in this Study

Gouge	Composition
Dry Lake Valley: 212–235 m depth interval of drill hole into the San Andreas near Hollister, Calif.	About 80% clays, 20% quartz + plagioclase. Approximate clay proportions: 50% montmorillonite + mixed-layer clays, 30% kaolinite, 10% chlorite, 10% illite
Serpentinite: from a trench in the San Andreas near San Carlos, Calif.	Clinochrysotile, lizardite, trace opaques
Illite: disaggregated illitic shale, from Fithian, Ill.	Approximately 70% illite, 20% quartz, 10% chlorite + kaolinite
Westerly granite: crushed sample from quarried material, R.I.	35% plagioclase, 25% quartz, 25% potash feldspar, 10% biotite + muscovite + chlorite, 5% opaques + alteration minerals (epidote, calcite, fluorite).

of changing the slip velocity on the strength and sliding stability of these four gouges. In addition, this paper contains the first petrographic description of the run products from both the earlier and present experiments. Along with temperature and gouge type, the slip rate was found to have some important controls on the deformation textures observed in these gouges. TCHALENKO (1970) and LOGAN et al. (1979), among others, have shown that many of the microscopic structures developed in laboratory experiments can be correlated with the regional structures of natural fault zones. Therefore, the relationships observed in this petrographic study may have application to the interpretation of fault-zone characteristics.

Experimental Procedure

Four gouges of differing composition were studied (Table 1); they were two clay-rich gouges, a serpentinite gouge, and a gouge composed of crushed Westerly granite. The montmorillonite-rich Dry Lake Valley gouge and the serpentinite gouge were natural fault-gouge materials collected from a drill hole and a trench, respectively, in the San Andreas fault. The granite gouge was representative of natural granitic and gneissic rock flours that have been found along the San Andreas fault zone in southern California (ANDERSON et al., 1980). The illite-rich sample provided a nonexpanding clay-bearing gouge for comparison with the montmorillonite-rich gouge. Identification of the clay minerals and estimation of their relative proportions in the Dry Lake Valley and illite-rich gouges (Table 1) were made by the procedure in SCHULTZ (1964). Mineral proportions in the granite gouge were determined from point counts of thin sections of the starting Westerly material. Serpentine mineral identifications were based principally on WHITTAKER and ZUSSMAN (1956), with

additional reference to the indexed diffraction lines of serpentine minerals in NEMECZ (1981) and the lizardite x-ray traces in BRINDLEY and ZUSSMAN (1957).

The experimental assembly is described in detail in MOORE et al. (1983). Briefly, each sample consisted of a layer of gouge 0.65 mm in thickness that was sandwiched between 30° finely ground saw-cut surfaces in a Westerly granite cylinder 19.0 mm in diameter and 41.3 mm long. The gouge-filled cylinder and insulating pieces were placed within an annealed copper jacket; the jacketed assembly was then placed in a cylindrically shaped resistance heater. All the experiments were run at a pore pressure of 30 bar, with deionized water as the pore fluid. Temperatures of 200, 400, and 600 °C and confining pressures of 1 and 2.5 kbar were tested. The temperature measurements were accurate to about ± 5 °C. The experiments were run at strain rates of 10^{-4}/sec and 10^{-6}/sec, which correspond to average sliding velocities along the saw cut of 4.8 and 4.8×10^{-2} μm/sec, respectively. These velocities refer to the average rate at which one granite piece slides past the other along the saw cut. For samples which show stick slip, velocities within the gouge layer will differ significantly between the stick and the slip portions of each cycle.

Confining and pore pressures were applied first to the jacketed sample. After these pressures had stabilized, the temperature was raised. The sample was held at temperature and pressure for 1800 sec before the load was applied. After completion of the experiments several of the run products were set aside for x-ray powder diffraction analysis. Thin sections of the remaining samples were prepared for standard petrographic analysis; each section was cut parallel to the long axis of the cylindrical sample and perpendicular to the plane of the fault gouge.

Results

Strength and sliding behavior

Plots of differential stress versus axial compression for the gouges at each temperature and sliding velocity studied are shown in Figures 1 to 3. The reproducibility of the results was verified in repeat experiments; some of the experiments at 600 °C and 2.5 kbar had to be repeated several times because of sample failures at these extreme conditions. For clarity, only one curve for each gouge has been plotted. As seen in these figures, the results at the two sliding velocities show very similar trends relative to temperature and confining pressure. Several of the curves at the slower slip rate are at slightly higher differential stresses than the corresponding experiments at the faster slip rate, but the results are essentially the same within the experimental variation.

At a given temperature and confining pressure at either sliding velocity, the three sheet-silicate-rich gouges supported roughly the same stresses. They and the granite gouge all showed increases in strength with increasing confining pressure. At 200 °C (Fig. 1) the granite gouge supported considerably higher stresses than the clay and
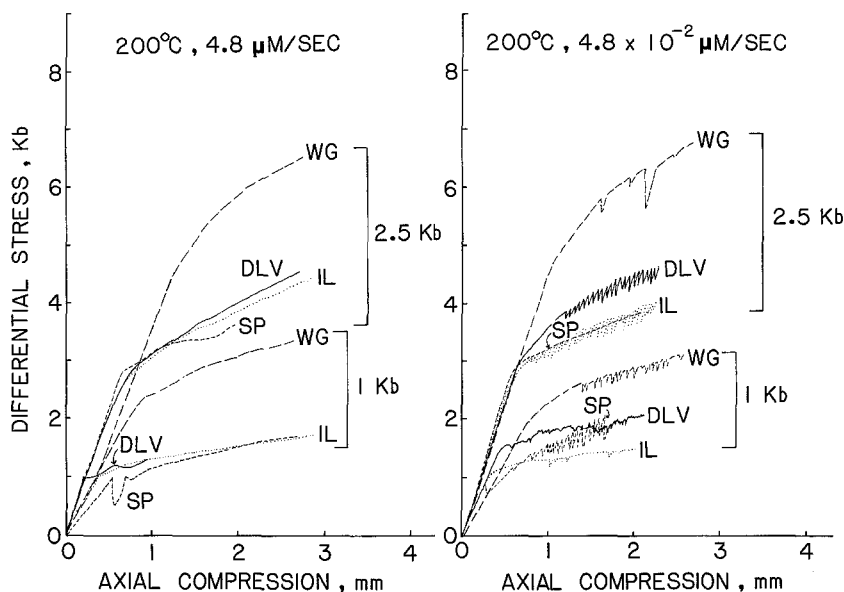
Figure 1
Plot of differential stress against axial compression for friction experiments at 200 °C, comparing results
at 4.8 and 4.8 × 10⁻² μm/sec sliding velocities: WG, Westerly granite gouge (long-dashed lines); DLV, Dry
Lake Valley gouge (solid lines); IL, illite gouge (dotted lines); SP, serpentinite gouge (short-dashed lines).

serpentinite gouges at both confining pressures. The strength of the granite gouge,
however, was unaffected by temperature, whereas the three sheet-silicate-rich gouges
showed marked strength increases with temperature. At 400 °C (Fig. 2) the granite
gouge was still stronger than the other gouges at 2.5 kbar, but all four gouges supported
similar stresses at 1 kbar. At 600 °C (Fig. 3) the clay and serpentinite gouge strengths
equalled that of the granite gouge at 2.5 kbar and surpassed it at 1 kbar.

In contrast to their strengths, the sliding behavior of the gouges did vary with
the sliding velocity (Figs. 1 to 3). At the 4.8 μm/sec slip rate the granite gouge slid
stably at all temperatures and pressures, and the three sheet-silicate-rich gouges slid
stably at 200 °C. At higher temperatures the clay-rich and serpentinite gouges had a
greater tendency to show stick slip, particularly at 1 kbar confining pressure. The
magnitude of the stress drops tended to increase with temperature. Reducing the
sliding velocity to 4.8 × 10⁻² μm/sec expanded the field of stick-slip behavior for
the sheet-silicate gouges to lower temperatures and higher confining pressures. In
addition, the granite gouge slid unstably in some of the experiments at the
4.8 × 10⁻² μm/sec slip rate. The differences in sliding stability at the two slip velocities
were particularly marked at 200 °C (Fig. 1). The size of the stress drops was also
slightly higher in the experiments at 4.8 × 10⁻² μm/sec. The best correlation between
slip rate and stress drop was seen in the 400 °C experiments (Fig. 2), but also at
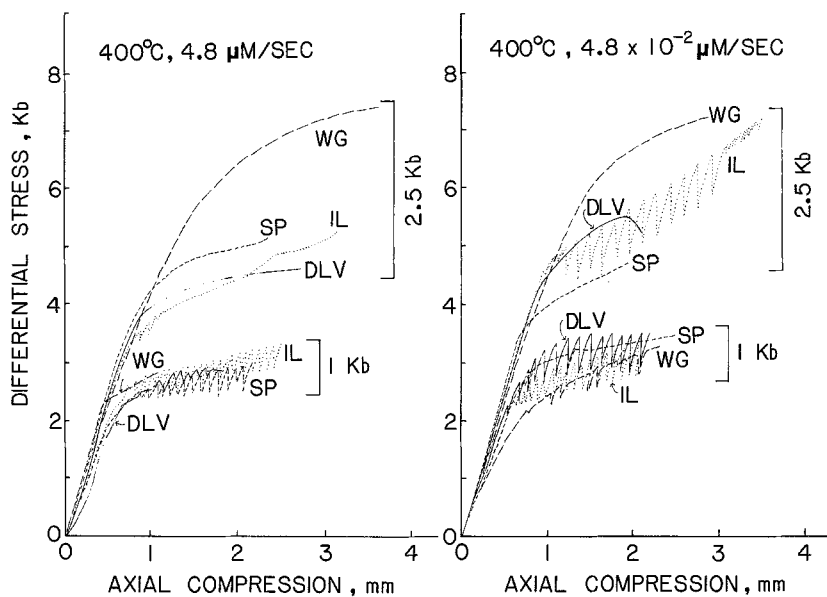
Figure 2

Frictional strengths of the four gouges at 400 °C and 4.8 and 4.8 × 10^{-2} μm/sec sliding velocities; same symbols as in Figure 1.
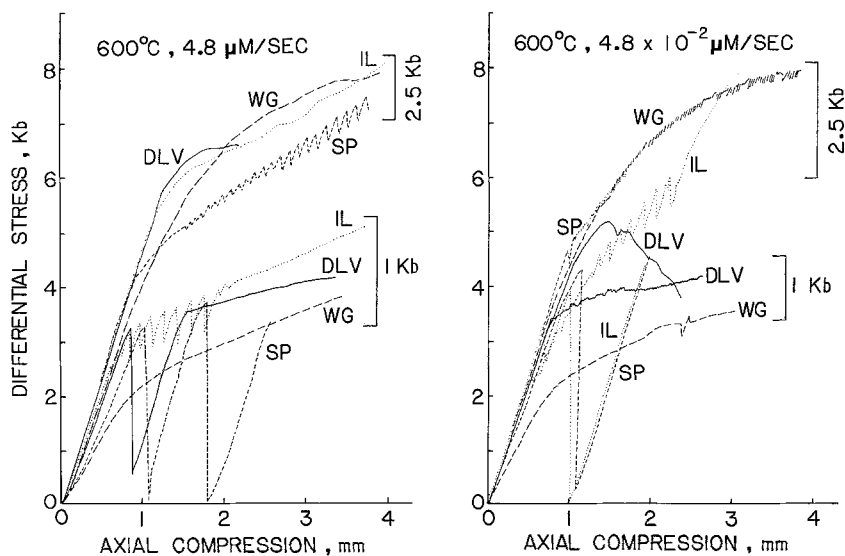

Figure 3

Strength plots, comparing results at 600 °C and 4.8 and 4.8 × 10^{-2} μm/sec sliding velocities; same symbols as in Figure 1.

600 °C the largest stress drops (approximately 4 kbar) were measured in the experiments at the slower displacement rate (Fig. 3).

Mineralogy

Samples of the starting material and run products of each gouge were prepared for x-ray diffraction analysis, by Cu K_α radiation, to establish the extent of mineral alteration during the experiments. The procedures are the same as described in MOORE et al. (1983); the results for the experiments at 4.8 μm/sec, along with representative diffraction patterns, also were described in MOORE et al. (1983). To summarize briefly the results at 4.8 μm/sec, the granite gouge showed almost no mineralogical changes with increasing temperature and pressure. The only visible effect was the gradual disappearance with temperature increase of the peaks for the minor alteration mineral chlorite. The x-ray peaks for clay minerals from the Dry Lake Valley and illite gouges generally decreased in intensity with temperature and pressure increase. Two exceptions were observed, however. The 10 Å illite peak was augmented at 600 °C because of the collapse of the dehydrated montmorillonite lattice from 14 to 10 Å. The 4.5 illite peak also increased in size, apparently because of modifications accompanying water loss from the illite structure.

Changing the sliding velocity to 4.8×10^{-2} μm/sec had no effect on the mineralogy of the granite gouge. The illite and Dry Lake Valley gouges did show some slight differences in the temperatures and pressures at which observable changes in the clay mineral peak intensities occurred. In addition, at 600 °C the intensities of the clay mineral peaks that decreased were somewhat lower in the experiments at the 4.8×10^{-2} μm/sec slip rate, and the intensities of the two peaks that increased were rather higher. No new mineral phases were observed in any of the run products of these three gouges.

Selected x-ray patterns at the two sliding velocities are shown for the serpentinite gouge in Figure 4. The serpentinite starting material was previously described (MOORE et al., 1983) as containing chrysotile as the sole serpentine mineral; the x-ray pattern, however, is more consistent with a combination of chrysotile and lizardite (Fig. 4), both of them low-temperature serpentine minerals. In contrast to the other gouges, the clinochrysotile and lizardite in some of the serpentinite gouge run products were replaced by new minerals; and the pressure and temperature conditions at which the reaction was observed varied somewhat with the slip rate. Every 600 °C sample at both sliding velocities contained forsteritic olivine instead of serpentine (Fig. 4). Poorly to well developed peaks attributable to talc also appeared at both confining pressures in the 600 °C x-ray traces, and some possible quartz peaks were present at 1 kbar. Serpentine was also partly or completely replaced by forsteritic olivine at a 400 °C, 1 kbar confining pressure and 4.8×10^{-2} μm/sec sliding velocity. The olivine peaks were less intense at 400 than at 600 °C, and no peaks appeared for either talc or quartz. The rest of the 400 °C samples showed no

evidence of olivine growth, although the serpentine mineral diffraction lines from those samples did have reduced intensities.

Petrography

The four gouges of this study offer a wide range of initial textures for petrographic comparison. The granite gouge consists of a framework of quartzofeldspathic grains ranging in size up to approximately 0.15 mm in diameter, with minor amounts of fine-grained, interstitial matrix. The illite-rich gouge, on the other hand, is almost completely composed of clay-sized material, with only a few silt- or sand-sized grains (maximum of 0.07 mm in diameter) of quartz and opaque minerals. The Dry Lake Valley gouge is intermediate between these two extremes; it contains many more quartzofeldspathic grains (maximum of 0.12 mm in diameter) than the illite gouge, but not enough to form a framework-grain-supported material. The serpentinite gouge texturally resembles the granite gouge, in that it consists predominantly of rounded grains of serpentine up to about 0.12 mm in diameter, which may be pseudomorphs of the original ultramafic minerals. This gouge therefore has a framework of coarse grains, but the serpentine grains are much softer than the quartzofeldspathic grains of the granite gouge.

Because the emphasis of this special volume is on 'fault zone' structures, the deformation textures of the run products will be described in some detail. Several similar schemes have been put forward for labeling the various fracture sets that have been identified in natural fault zones and in the products of gouge friction and shear box experiments (e.g., SKEMPTON, 1966; TCHALENKO, 1968, 1970; TCHALENKO and AMBRASEYS, 1970; LOGAN et al., 1979). The terminology of LOGAN et al. (1979), which is illustrated in modified form in Figure 5, was adopted for this study because their scheme was the only one used for describing the run products of gouge friction experiments. The other schemes describe fracture sets with the same orientations and offset directions as shown in Figure 5, but they employ slightly different letter labels (e.g., the Y fractures in Figure 5 are labeled 'D' by TCHALENKO, 1968). For convenience in reporting, the letter scheme in Figure 5 has been used for describing not only the relative orientations of fracture and fault planes but also the orientations within the plane of the thin section of features such as kink bands and aligned minerals. This does not necessarily mean that the latter features will have the same orientation in the third dimension as the fault planes.

Granite gouge. Of the four gouges examined the crushed granite gouge shows the greatest variety of deformation textures. At 200 and 400 °C a series of low-angle R1 fractures that cross-cut the gouge layers are among the most prominent features in the samples. Individual grains that are split by the fractures show offsets of up to 0.05 mm (Fig. 6a). Opaque and phyllosilicate minerals are commonly smeared out along the fracture traces. At 600 °C the R1 traces are much more closely spaced, but
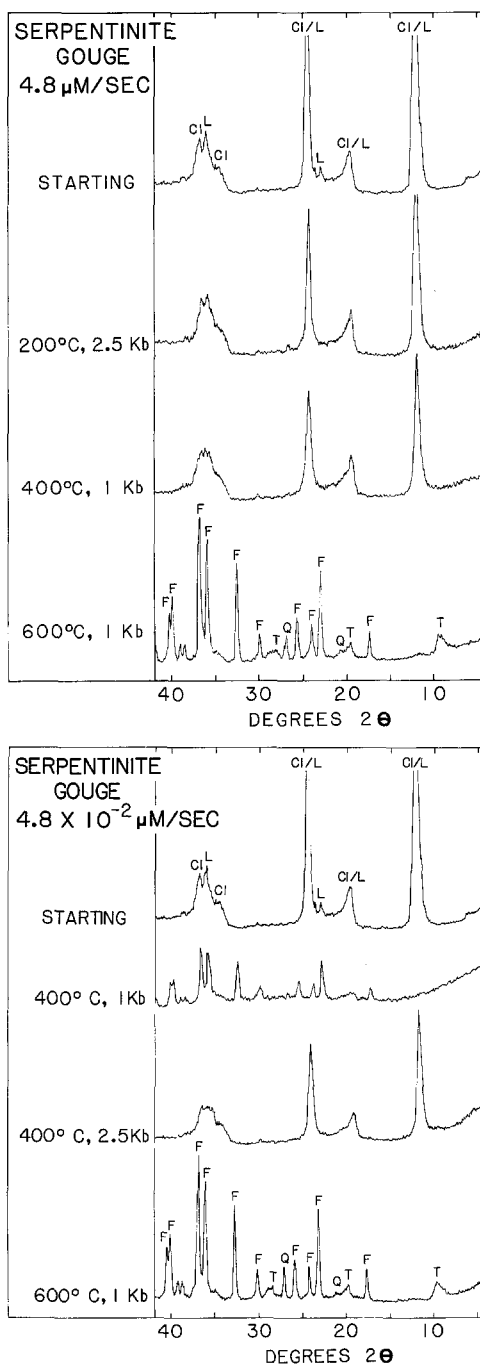
Figure 4

X-ray diffraction patterns of serpentinite gouge starting material and run products at 4.8 and 4.8 $\times$ 10^{-2} μm/sec sliding velocities: Cl, clinochrysotile; L, lizardite; F, forsteritic (Mg-rich) olivine; T, talc; Q, quartz. Cu K_α radiation.
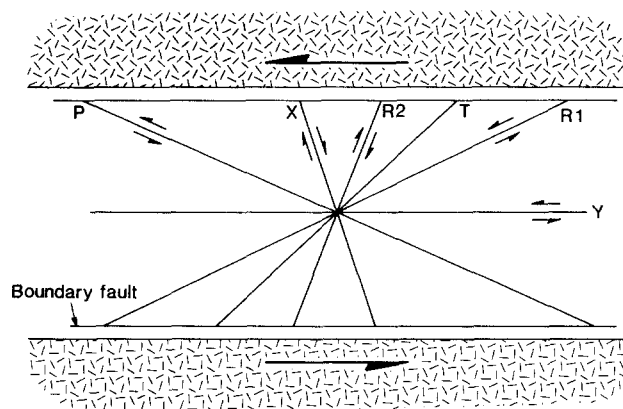
Figure 5
Labeling scheme of LOGAN et al. (1979, p. 325–6) for fracture sets developed in gouge layers deformed in triaxial friction experiments. The terminology of LOGAN et al. is used in this paper. The orientation of this diagram is the same at that of the examined thin sections, that is, parallel to the long axis of the cylindrical sample and perpendicular to the plane of the fault gouge.

individual planes are less well defined than at lower temperatures. The angle between the R1 fractures and the edge of the gouge layer ranges from 6° to 19°; the range is 6° to 11° for the samples with 4.8 μm/sec sliding velocity and 9° to 19° for the samples at 4.8 × 10^{-2} μm/sec. Cross-cutting fracture sets with different orientations were not observed, though a few individual quartz and feldspar grains in the gouge show fractures and offsets consistent with the R2 fractures.

The R1 fractures terminate at a fracture that is oriented parallel to the edge of the gouge layer and that is located at or within about 0.1 mm of the boundary (Fig. 6b). These boundary fractures commonly are filled with a very fine-grained grayish-brown material; in places, smeared-out phyllosilicate or opaque grains can be identified in the fracture filling. Some of the smeared grains were plucked from the adjoining granite cylinder. A boundary fracture is developed to at least some extent on both sides of every granite gouge sample, but it is generally more continuous on one side than on the other. The principal boundary fracture is usually straight, whereas the subsidiary one may have a jagged trend, with some of the segments extending into R1 fractures (Fig. 6b). In the samples at 600 °C and a 2.5 kbar confining pressure, short segments of the boundary fractures cut through the rock cylinder rather than the gouge. The slices of rock trapped within these segments have been partly crushed. In the 600 °C samples run at the faster sliding velocity, the granite cylinder adjacent to the gouge layer contains a number of short fractures oriented at angles between 0° and 45° to the gouge–rock boundary.

The granite gouge shows increasing degrees of grain-size reduction with increasing temperature and confining pressure. At 200 and 400 °C the zones of most
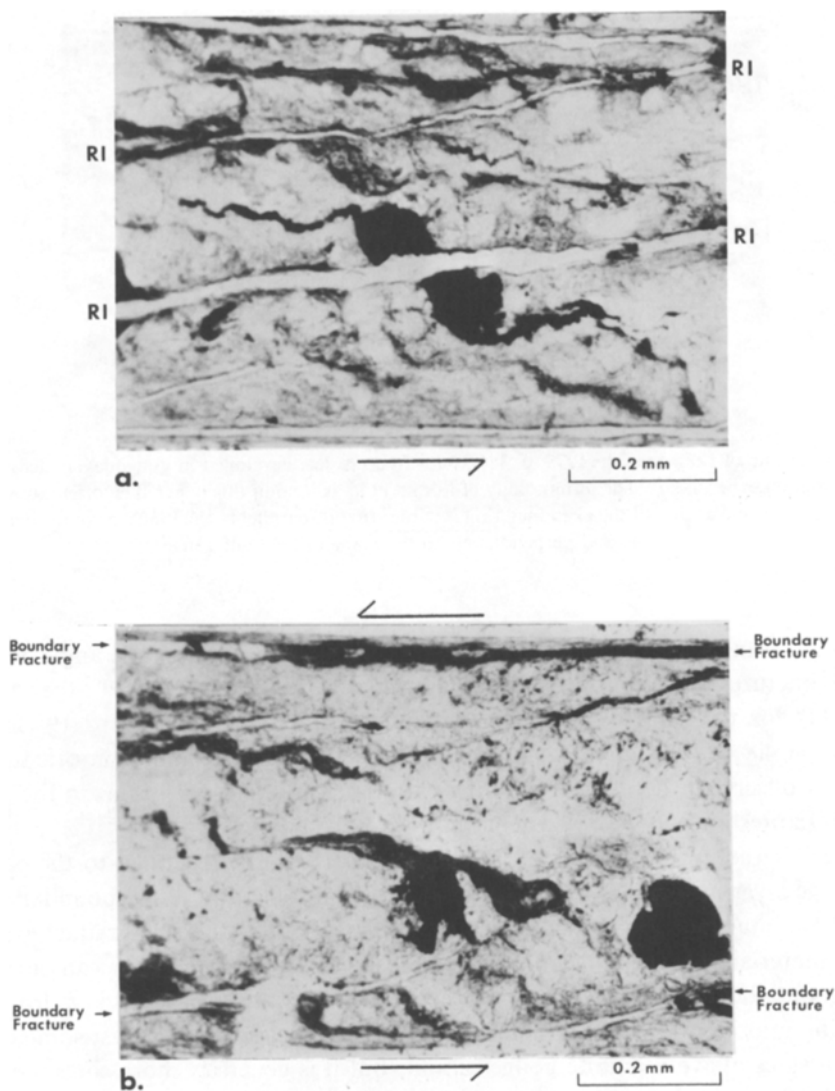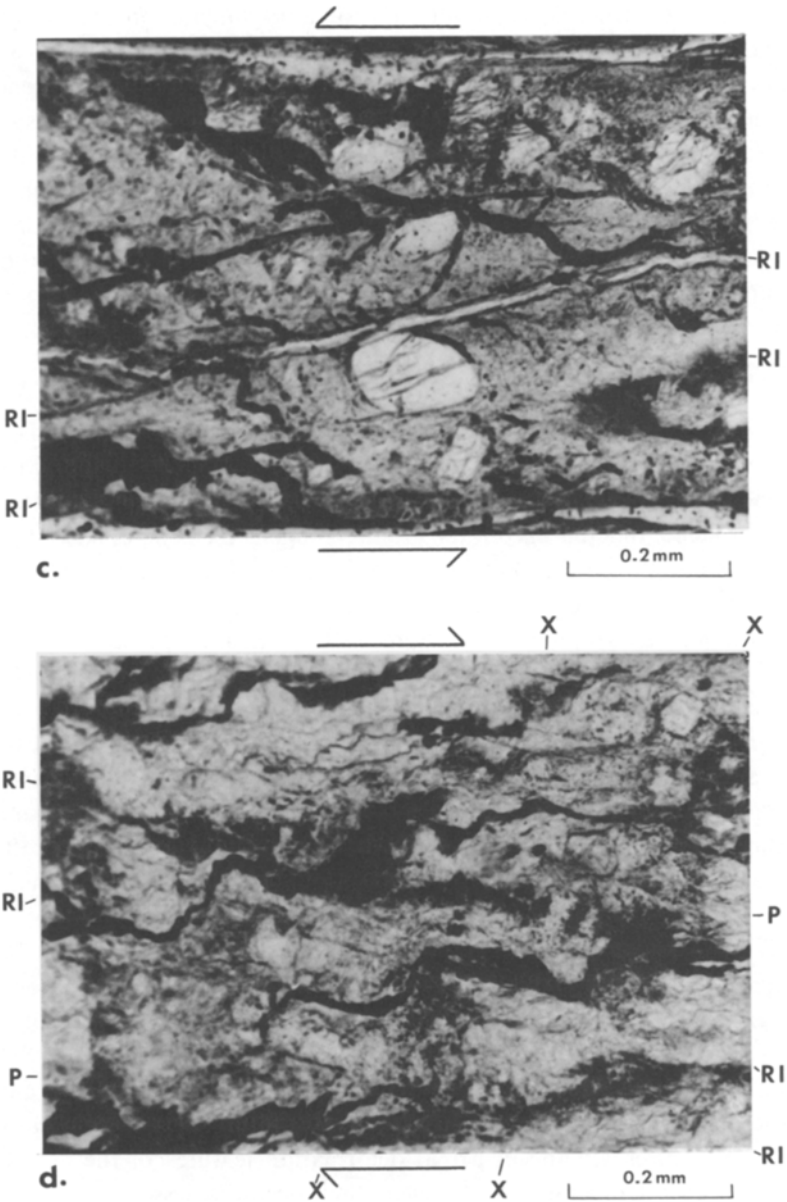
Figure 6
Textures of heated granite gouge. (a) Opaque grain offset along an R1 fracture. Note the tails of opaque material extending from each half of the opaque grain. The shear direction is as indicated in the figure (sample at 400 °C and 1 kbar confining pressure) (b) Examples of boundary fractures. The fracture at the top of the gouge layer is relatively straight and filled with fine-grained, dark material. The fracture at the base consists of a set of short segments that terminate in R1 fractures. Much of the fine-grained filling of the lower boundary fracture was lost during the thin-sectioning process (400 °C, 1 kbar). (c) An otherwise well-rounded quartz clast with flattened surfaces along R1 fractures. This grain also contains internal fractures aligned roughly in the R1 direction (400 °C, 1 Kbar). (d) Opaque and phyllosilicate grains deformed in a stepwise manner in the R1 and X directions (600 °C, 2.5 kbar). All four photos are in plane-polarized light; all four show the entire width of the gouge layer.

c.   0.2mm

d.   0.2mm

intense grain crushing show no particular relationship to other deformation textures in the gouge, with the exception of otherwise rounded grains that have flattened surfaces adjacent to the R1 fractures (Fig. 6c). However, the 600 °C gouge samples contain alternating bands of coarser and more finely grained material that are bounded by the R1 planes.

The abundant dark-colored biotite and opaque minerals in the granite gouge provide good indicators of grain deformation. These grains characteristically occur as 'ductile stringers' (LOGAN et al., 1981, p. 130) that have an overall orientation in the P direction (Figure 6d). In detail, however, the deformed grains consist of long segments on adjacent R1 planes that are connected by shorter segments parallel to X. At lower temperatures this stepwise, segmented appearance is well defined, but in the more highly deformed, 600 °C samples the changes in orientation are less abrupt and the deformed opaques and phyllosilicates have an undulating appearance. The number and amount of strain of these deformed grains increases with temperature; at 600 °C this mineral fabric is much more pronounced in the samples run at the faster sliding velocity.

Dry Lake Valley gouge. In general, the Dry Lake Valley gouge contains the same types of deformation texture as the granite gouge, but they are developed to a lesser degree. Because of this the Dry Lake Valley gouge has a relatively massive appearance. The principal difference from the granite gouge is the general lack of grain-size reduction, resulting from the isolation of the larger grains of quartz and feldspar in soft, clayey matrix. Some quartz and feldspar grains, however, are offset along breaks that have the R2 fracture orientation. Some of the larger grains are deformed in the same stepwise manner as that described for the granite gouge; such strained grains are more common in the samples at the 4.8 μm/sec sliding velocity.

The Dry Lake Valley gouge also contains low-angle R1 fractures and boundary faults. In a 600 °C sample the boundary fault along one side of the gouge layer is discontinuous, terminating where it intersects an R1 fracture. As was observed with the granite gouge, the angle between the R1 fractures and the edge of the gouge layer varies with the sliding velocity: at 4.8 μm/sec the angle ranges from 8° to 15°, and at 4.8 $\times$ 10^{-2} μm/sec it is between 14° and 23°.

Illite gouge. The illite gouge contains a rather different set of deformation textures from the granite and Dry Lake Valley gouges. For example, the 200 °C illite samples contain cross-cutting fractures with a variety of orientations. Fractures with the T orientation (40–55°) predominate, and R2 fractures (65–70°) are also common; R1 and X fractures are less abundant. The gouge adjacent to the fractures generally is compacted. Fractures are the principal deformation features of the 200 °C gouge samples; at higher temperatures, however, they occur in lesser numbers and are generally oriented in the R1 direction. The R1 fracture angles are 6° to 15° for the samples at a sliding velocity of 4.8 μm/sec and 11° to 33° for those at 4.8 $\times$ 10^{-2} μm/sec.

The 400 and 600 °C illite samples contain kink bands that are oriented approximately parallel to the R1 fractures (10° to 17°). The clay minerals in the narrow, kinked portions are aligned parallel to the edge of the gouge layer. The clays in the wider zones between the kinks are aligned parallel to P. In some samples the kink
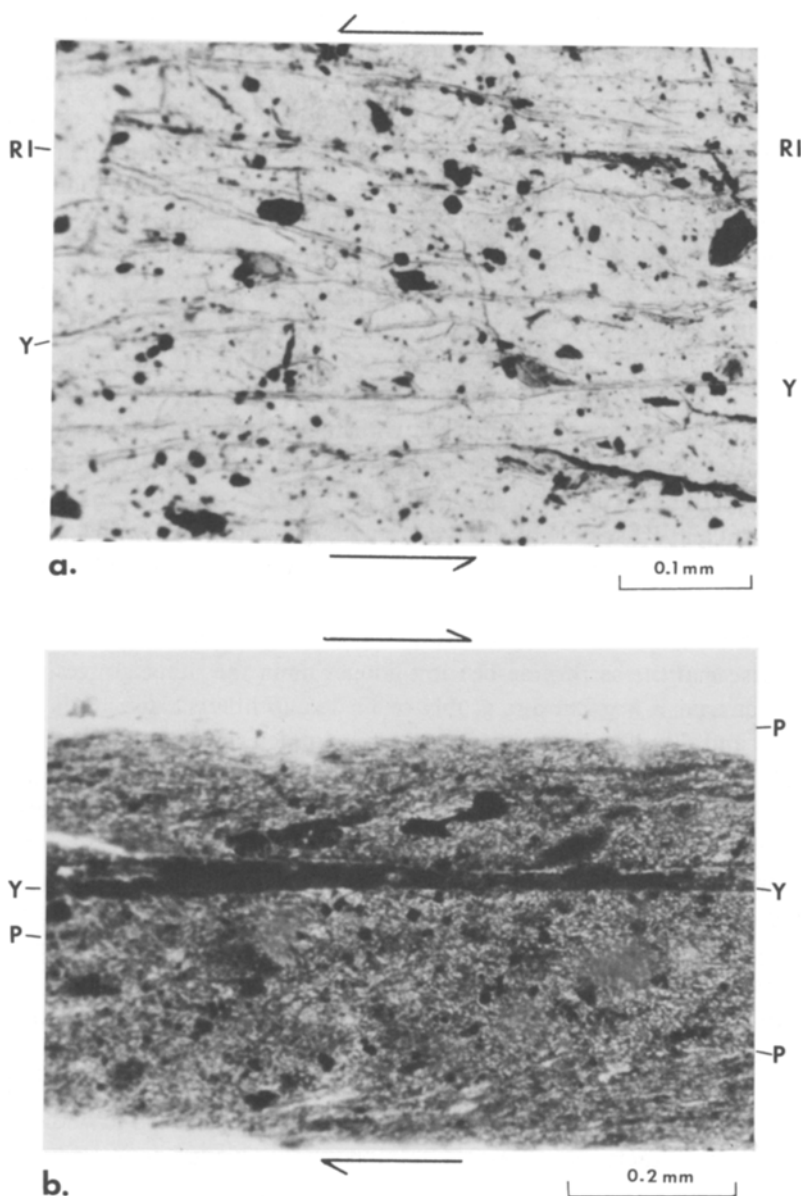
Figure 7

Textures of heated serpentinite gouge, in plane-polarized light. (a) Serpentine-bearing sample, at 200 °C and 2.5 kbar, showing Y and R1 fractures. In the center a serpentine grain is offset along a Y fracture. (b) Olivine-bearing sample at 600 °C and 2.5 kbar. The gouge consists principally of small, rounded crystals of brownish-colored olivine; the lighter-colored interstitial areas are talc. A fracture filled with dark, fine-grained material lies roughly parallel to the boundary of the gouge layer but well within the gouge. The upper third of the gouge layer contains some relict opaque grains stretched in the P direction. In the lower right-hand corner a faint lamination, also in the P direction, is visible.

bands extend only partway across the gouge layer from one side, whereas in others they transect the entire gouge layer.

Opaque grains in the 600 °C illite samples have been strained; most of them are elongate parallel to P, although a few are nearly parallel to the gouge–rock boundary. The illite gouge samples also contain the boundary faults filled with isotropic material that were observed in the other two gouges. One 600 °C sample has a boundary fault on only one side, and a second 600 °C sample has two, closely spaced boundary faults along part of one side.

Serpentinite gouge. The 200 and 400 °C serpentine-bearing samples contain intersecting sets of Y and R1 fractures (Fig. 7a). The Y fractures characteristically have a wavy appearance and are discontinuous; some serpentine grains cut by the Y fractures are slightly offset in accordance with the shear direction (Fig. 7a). Many other serpentine grains have been crushed and smeared out along the fractures. Fine-grained serpentine in the zones between fractures shows a faint extinction alignment parallel to X. Some of the remaining large serpentine grains contain kink bands that also are oriented in the X direction. Some red-colored phyllosilicate grains and opaque minerals that are present in the starting serpentinite gouge have been strained parallel to P. Boundary fractures filled with fine-grained material are not as common in the serpentine-bearing gouges as in the other gouges examined; some samples have a fracture along only one side and others none at all.

The 400 and 600 °C olivine-bearing gouge samples show a combination of deformation and crystallization textures. The 400 °C olivine-bearing sample preserves the original serpentine fabric to a large degree, but the edges of the grains are poorly defined. These relict clasts have a dusty appearance, not seen in the serpentine-bearing samples, that may be very fine-grained olivine. In one 600 °C sample olivine occurs as a series of small, round, brownish-colored crystals that form around the edges of relict serpentine grain shapes. With increasing amounts of olivine growth the relict grain shapes gradually disappear, and at the extreme case the gouge consists of a mat of small, round, brownish-colored olivine crystals with minor amounts of interstitial talc and quartz (Fig. 7b).

The olivine-bearing gouges principally contain R1 fractures (14° to 22°) and boundary fractures, although some T fractures (40°) were observed in one sample. In place of boundary fractures one 600 °C sample contains a single Y fracture that is located about a third of the way across the layer (Fig. 7b). Some of the relict serpentine grain shapes in the 400 °C olivine-bearing sample are offset along R1 fractures, whereas others are flattened in the Y planes. The 400 °C sample also contains somewhat wavy kink bands that are oriented roughly perpendicular to the gouge–rock boundary. One 600 °C sample contains laminae parallel to P that extend partway into the gouge from the edge (Fig. 7b). Strained opaque grains also are elongate in the P direction.

Discussion

Strength and sliding stability

The effects of temperature and confining pressure on the frictional properties of these four gouges were considered in MOORE et al. (1983); this discussion will concentrate principally on the effects of changing the sliding velocity. Few studies of rock or gouge friction have dealt with changing displacement rates. Of these, OLSSON (1974), ENGELDER et al. (1975), and TEUFEL and LOGAN (1978) found no dependence of friction strength on slip rate. By contrast, DIETERICH (1981) varied the sliding velocity of the same sample of granite gouge during direct shear experiments, and he found that decreasing the sliding velocity produced a slight increase in the residual strength of the gouge. Dieterich's results are consistent with the observation in our experiments that many of the curves at the slower slip rate plotted at slightly higher differential stresses. TEUFEL and LOGAN (1978) observed a relationship between sliding velocity and sliding stability similar to that reported here; during room-temperature friction experiments on cut specimens of Tennessee sandstone they reported a change from stable sliding to stick slip as the sliding velocity was lowered. ENGELDER et al. (1975) found that at slower sliding rates the size of the stress drops was larger for samples of quartz gouge showing stick slip; this also corresponds to the relationships in Figures 1 to 3.
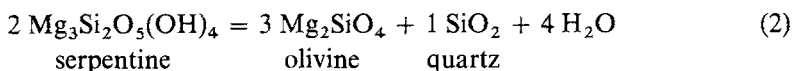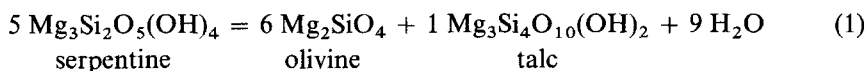
The correlation between slip rate and stick slip in room-temperature friction experiments on gouge has been explained as a result of the interlocking of grains in the gouge (SUMMERS and BYERLEE, 1977). As a gouge becomes more highly compacted, sliding must take place by fracturing through grains rather than over them. MOORE et al. (1983) proposed a similar mechanism for the increase in the occurrence of stick slip in the sheet-silicate-rich gouges with increasing temperature. The clay-rich and serpentinite gouges showed greater degrees of lithification at higher temperatures, and sliding would then have occurred by fracturing through the hardened mineral aggregate. Decreasing the sliding velocity would also promote lithification and thereby stick-slip behavior in these three gouges, because of the concomitant increase in heating time.

In the experiments at 4.8 μm/sec the granite gouge was compacted but not lithified (MOORE et al., 1983). Because of this, the occurrence of stick slip during some of the granite gouge experiments at 4.8×10^{-2} μm/sec may be due simply to increased compaction of this gouge at the slower deformation rate; but lithification may also be a factor in the lower-velocity experiments. Given enough time, cementation lithification of quartz-bearing gouges could occur through solution and redeposition of silica from pore fluids (ANGEVINE et al., 1982). This process may have occurred to some extent in the experiments at the slower displacement rate with their longer reaction times. Cementation of the granite gouge probably was not very extensive even at the slower slip rate, however, because less than half of the granite samples showed stick slip at that displacement rate and the run products were also not visibly lithified.

Mineralogical changes

As described previously, the x-ray patterns of quartz and feldspar minerals in the gouges were unaffected by changes in the sliding velocity. The effects on the clay mineral x-ray intensities were also not particularly significant. Many clay minerals begin to lose some of their loosely bound water at temperatures between 100 and 200 °C (DEER et al., 1962), so that the temperature conditions of all the friction experiments of this study were within the field of clay mineral dehydration. At any given temperature and pressure the dehydration reactions were more thorough at the slower sliding velocity, but this difference is readily explained by the corresponding increase in the amount of heating time (e.g., BRINDLEY and ZUSSMAN, 1957).

In contrast to the clays, the lowest temperature at which an olivine-forming reaction in the serpentinite gouge was observed did vary with the sliding velocity (Fig. 4). On the basis of the mineral assemblages observed in the x-ray patterns (Fig. 4) and in thin section, the lizardite and chrysotile of the serpentinite gouge reacted at 600 °C as follows:

$$5\,Mg_3Si_2O_5(OH)_4 = 6\,Mg_2SiO_4 + 1\,Mg_3Si_4O_{10}(OH)_2 + 9\,H_2O \qquad (1)$$
$$\text{serpentine} \qquad \text{olivine} \qquad \text{talc}$$

$$2\,Mg_3Si_2O_5(OH)_4 = 3\,Mg_2SiO_4 + 1\,SiO_2 + 4\,H_2O \qquad (2)$$
$$\text{serpentine} \qquad \text{olivine} \qquad \text{quartz}$$

One of these two reactions is probably also responsible for the appearance of olivine in the slower sliding-velocity experiments at 400 °C, even though neither quartz nor talc appeared with olivine in the 400 °C x-ray traces. As seen in Figure 4b, the x-ray peaks for olivine are much weaker at 400 than at 600 °C. A similar reduction in the talc or quartz x-ray intensities at 400 °C could reduce them to the level of the background noise. Typically, a mineral must be at least 5 to 10 percent of a sample to appear on an x-ray pattern.

Of the two, reaction (1) is the more likely to have occurred at 400 °C. Reaction (2) takes place in air at temperatures near 600 °C (DEER et al., 1962), and at the higher confining pressures of the friction experiments the reaction would probably shift to slightly higher rather than to lower temperatures. In the phase diagram for the system MgO–SiO_2–H_2O of EVANS et al. (1976), part of which is shown in Figure 8, reaction (1) is located at about 430 °C at 1 kbar of confining pressure and at about 450 °C at 2.5 kbar. Such temperatures are also slightly too high to explain the observed 400 °C results for the serpentinite gouge. EVANS et al. (1976), however, described some uncertainties in applying the existing experimental data for reaction (1) to their diagram, which they resolved by consideration of field evidence. Therefore, the placement of reaction (1) in their diagram is not completely certain; it may occur at slightly lower temperatures than shown. In addition, the phase diagram of EVANS et al. (1976) was constructed for conditions of $P_{conf} = P_{fl}$ whereas in the
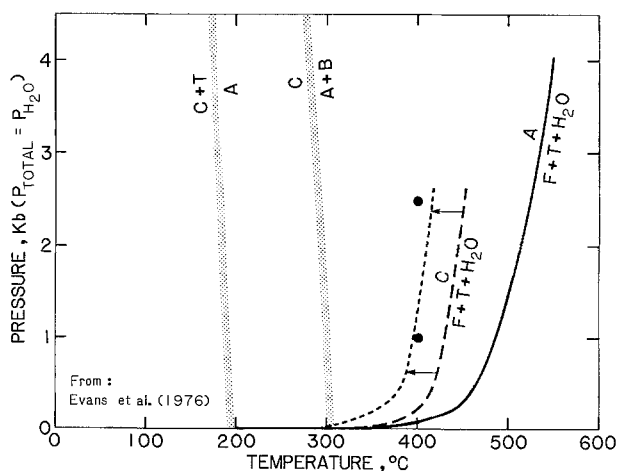
Figure 8

A portion of the phase diagram of EVANS et al. (1976) for the system MgO–SiO₂–H₂O: C, chrysotile; T, talc; A, antigorite; B, brucite; F, forsterite. Reaction (1) is metastable in this system, and reaction C = A + B would be the stable reaction for the 400 °C serpentinite gouge experiments. This reaction, however, is sluggish both in nature and in the laboratory. Reaction (1)′ indicates a possible position for Reaction (1) at low fluid pressures, which would allow olivine to form in the gouge experiments at 400 °C and 1 kbar confining pressure.

friction experiments $P_{conf} \gg P_{fl}$. At lower fluid pressures relative to confining pressure, the reaction should be displaced to slightly lower temperatures. A shift of Reaction (1) to Reaction (1)′ in Figure 8 would be sufficient to make the serpentine-forming reaction possible at 400 °C and a 1 kbar confining pressure.

Assuming that the placement of reaction (1)′ in Figure 8 is approximately correct, the restricted occurrence of the olivine-forming reaction to the slower-velocity experiments at 400 °C and a 1 kbar confining pressure may be due to the combined effects of deformation and increased reaction time. Although the reaction theoretically could occur at those temperature–pressure conditions, sluggish reaction kinetics at such relatively low metamorphic temperatures might inhibit the breakdown of serpentine even at relatively long times during hydrostatic experiments. This was tested by heating of a serpentinite gouge sample for 66 hours at 400 °C and a confining pressure of 1 kbar, without an axial load being applied. Although the amount of time in this experiment was considerably greater than that for an experiment at a sliding velocity of 4.8 × 10⁻² μm/sec, no evidence of reaction was found. An increase in the strain and surface energy of the serpentine grains during deformation may have promoted the reaction to the extent that it is observable in the longer experiments.

Gouge textures

Many of the textures observed in the gouges are functions of the initial physical character of the gouges. The relative amounts of hard and soft grains, in particular, control the development of cataclastic textures and kink bands in the gouges. A relationship also exists between gouge type and fracture development, for example, the restriction of Y fractures to the serpentine-bearing and olivine-bearing gouges, and the many different fracture orientations in the low-temperature illite gouge samples. Temperature and confining pressure also have important effects on gouge texture, including the amount of grain-size reduction and the degree of induration of a given gouge.

Of particular interest in this discussion are the relationships between sliding velocity and gouge textures. Perhaps the most significant correlation is the increase in the R1 angles with decreasing displacement rate, which was observed for three of the gouges. The physical significance of the R1 fracture orientations has been considered by a number of workers, particularly those involved in soil mechanics research (e.g., RIEDEL, 1929; HANSEN, 1961; TCHALENKO, 1970; see discussion in MORGENSTERN and TCHALENKO, 1967). The results of many of the shear box tests and Riedel experiments have been interpreted on the assumption that the deformation is of the simple shear type; in such a case the following relationship should hold:

$$\theta' = \varphi/2 \qquad (3)$$

where θ' is the angle between the R1 fracture and the direction of shear, and φ is the angle of internal friction (HANSEN, 1961; TCHALENKO, 1970). Using this equation, TCHALENKO (1970) has reported that the fracture angles developed during shear box tests on kaolin, bentonite, and London Clay yielded angles of internal friction consistent with the experimentally determined values for those clays. Equation (3) also is valid for room-temperature triaxial friction tests. For example, LOGAN et al. (1979) found a close agreement between coefficients of friction of pure quartz gouge obtained from equation (3) and from strength measurements. BYERLEE et al. (1978) reported R1 angles for room-temperature experiments on quartz gouge that were consistent with those of LOGAN et al. (1979). The two sets of results for quartz gouge covered a range of sliding velocities, which indicates the lack of a velocity relationship at room temperature. Equation (3) also appears to work reasonably well for the subsidiary R1 fractures developed in surface sediments during a recent earthquake in Iran (TCHALENKO and AMBRASEYS, 1970).

On the basis of these results, the observed correlation between sliding velocity and R1 angle in the heated gouge samples would not be predicted from the strength measurements. Instead, all the granite gouge samples would be expected to have the same R1 angles, whereas the clay-rich and serpentinite gouges should show a change in R1 angle with temperature because of the pronounced temperature-related

changes in the coefficients of friction for these three gouges (MOORE et al., 1983, Fig. 8, p. 495). In contrast to our results, LOGAN et al. (1979) did find a decrease with increasing temperature in both the strength and the R1 angles of calcite gouge.

The origin of the sliding-velocity relationship in the experiments of this study is as yet unknown. The increase in R1 angle with decreasing slip velocity is consistent with observations of DIETERICH (1981) in room-temperature experiments, that gouge strength was inversely related to sliding velocity. However, a velocity relationship to strength could not definitely be proved in the experiments of this study. One possible explanation of the high-temperature R1 angles is that at least one of the assumptions used in analyzing the room-temperature shear box and friction experiment data is not applicable at high temperatures. Alternatively, some additional factors may have to be considered for the heated gouge samples, such as changes in the degree of cohesion of the clay and serpentinite gouges at elevated temperatures. Further work needs to be done to elucidate the origin of the fracture-angle variations and to identify any other controlling factors.

Because stick-slip motion in triaxial friction tests has been correlated with earthquakes in nature (BYERLEE, 1970), it is important in earthquake-prediction programs to identify the causes of stick-slip behavior. On the basis of room-temperature friction studies of quartz gouge ENGELDER et al. (1975) and BYERLEE et al. (1978) proposed that the onset of stick slip corresponds to a shift in slip from the cross-cutting (R1) faults to the boundary faults. For the four heated gouges of this study, however, both types of fracture were observed in samples that slid stably as well as in ones that showed stick slip. SHIMAMOTO (1977) also found that slip was concentrated along the gouge–rock interface for room-temperature quartz and dolomite gouges that slid stably. Therefore, the development of boundary faults cannot be correlated with stick slip. In this study a decrease in sliding velocity has been related to an increase in the frequency of stick slip and also to an increase in R1 fracture angle. From this one might predict an additional correlation between high R1 angle and the occurrence of stick-slip motion. At the present time, however, this additional relationship is not confirmed, because stably and unstably sliding samples of a particular gouge at a given displacement rate had similar R1 angles. The number of samples examined petrographically for this study, however, was relatively small. Many more thin sections from other experiments are at present being prepared for further tests for this relationship and for other physical manifestations of stick slip.

The observed relationship between sliding velocity and fracture angle may have a potential use in estimations of the relative slip rates of fault zones. Fracture sets equivalent to the experimental R1 fractures have frequently been observed in natural fault zones (e.g., TCHALENKO and AMBRASEYS, 1970; LOGAN et al., 1979). Because the change in fracture angle occurs for a variety of compositions of heated gouge, this tool may be applicable at least to those portions of a fault that have been subjected

to elevated temperatures.

Another potential slip-rate indicator for heated gouges is the amount of grain deformation. In the granite and Dry Lake Valley gouge samples examined, strained and elongated grains were more common and had higher aspect ratios in the experiments at a sliding velocity of 4.8 μm/sec. The results of LOGAN et al. (1981) for strength experiments at 300 °C with the Dry Lake Valley gouge are also consistent with those reported here. Quartz and feldspar clasts in their run products, which were deformed at a 10^{-2}/sec strain rate, or roughly 5.1×10^2 μm/sec displacement rate along the saw cut, were considerably stretched (see Fig. 15 of LOGAN et al., 1981, p. 132). In this study the samples of Dry Lake Valley gouge tested at the 4.8 μm/sec sliding velocity contained only a few slightly strained quartz and feldspar grains, although some opaque and phyllosilicate grains were relatively strongly deformed. At 4.8×10^{-2} μm/sec almost none of the grains in the Dry Lake Valley gouge were deformed.

The mineral fabric may prove to be a relatively poor indicator of slip rates in high-temperature fault zones, because many factors besides displacement rate may probably affect the degree of grain deformation. The age of the fault and the total amount of displacement along it may be particularly significant controls on the deformation texture. Fluid pressure may also be important (LOGAN et al., 1981). Additional experiments need to be conducted for assessment of the significance of these other factors.

Conclusions

Changing the sliding velocity has been found to have several effects on the frictional and physical properties of heated fault gouge. At the slower slip rate (a) the gouges showed a greater tendency to stick-slip motion, and individual stress drops tended to be larger, (b) observable replacement of serpentine minerals by olivine was found at a lower temperature, (c) the angle between low-angle Riedel (R1) fractures and the boundary of the gouge zone was higher, and (d) grain deformation was less pronounced at a given temperature and pressure.

The mineralogical effect may have resulted from a combination of deformation and increased reaction time at the slower slip rate. The observed relationships between sliding velocity and sliding stability may have important applications in determinations of the conditions under which earthquakes occur at depth in fault zones. The textual variations relative to the sliding velocity may have potential application in determinations of the relative slip rates of natural fault zones.

REFERENCES

ANDERSON, J. L., OSBORNE, R. H. and PALMER, D. F. (1980), *Petrogenesis of cataclastic rocks within the San Andreas fault zone of southern California*. Tectonophys. *67*, 221–249.

ANGEVINE, C. L., TURCOTTE, D. L. and FURNISH, M. D. (1982), *Pressure solution lithification as a mechanism for the stick-slip behavior of faults*. Tectonics. *1*, 151–160.

BRACE, W. F. and BYERLEE, J. D. (1970), *California earthquakes: Why only shallow focus?*. Science. *168*, 1573–1575.

BRINDLEY, G. W. and ZUSSMAN, J. (1957), *A structural study of the thermal transformation of serpentine minerals to forsterite*. Amer. Min. *42*, 461–474.

BYERLEE, J. D. (1970), *The mechanics of stick-slip*. Tectonophys. *9*, 475–486.

BYERLEE, J., MJACHKIN, V., SUMMERS, R. and VOEVODA, O. (1978), *Structures developed in fault gouge during stable sliding and stick-slip*. Tectonophys. *44*, 161–171.

DEER, W. A., HOWIE, R. A. and ZUSSMAN, J., *Rock-forming minerals, Vol. 3: Sheet Silicates.* John Wiley, New York, 1962, p. 170–190.

DIETERICH, J. H. (1981), 'Constitutive properties of faults with simulated gouge', in N. L. Carter, M. Friedman, J. M. Logan and D. W. Stearns (eds.), *Mechanical Behavior of Crustal Rocks.* Amer. Geophys. Union Geophys. Mon. *24*, 103–120.

ENGELDER, J. T., LOGAN, J. M. and HANDIN, J. (1975), *The sliding characteristics of sandstone on quartz fault gouge.* Pure Appl. Geophys. *113*, 69–86.

EVANS, B. W., JOHANNES, W., OTERDOOM, H. and TROMMSDORFF, V. (1976), *Stability of chrysotile and antigorite in the serpentinite multisystem.* Schweiz. Min. Petrogr. Mitt. *56*, 79–93.

HANSEN, B. (1961), *Shear box tests on sand.* Proc. Fifth Internat. Conf. Soil Mech. *1*, 127–131.

LOGAN, J. M., FRIEDMAN, M., HIGGS, N., DENGO, C. and SHIMAMOTO, T. (1979), *Experimental studies of simulated gouge and their application to studies of natural fault zones.* Proc. Conf. VIII, Analysis of Actual Fault Zones in Bedrock, U.S. Geol. Surv. Open-File Rept. *79–1239*, 305–343.

LOGAN, J. M., HIGGS, N. G. and FRIEDMAN, M. (1981), 'Laboratory studies on natural gouge from the U.S. Geological Survey Dry Lake Valley No. 1 well, San Andreas fault zone', in N. L. Carter, M. Friedman, J. M. Logan and D. W. Stearns (eds.), *Mechanical Behavior of Crustal Rocks.* Amer. Geophys. Union Geophys. Mon. *24*, 121–134.

MOORE, D. E., SUMMERS, R. and BYERLEE, J. D. (1983), *Strengths of clay and non-clay fault gouge at elevated temperatures and pressures.* Proc. 24th U.S. Symp. Rock Mech., 489–500.

MORGENSTERN, M. R. and TCHALENKO, J. S. (1967), *Microscopic structures in kaolin subjected to direct shear.* Geotechn. *17*, 309–328.

NEMECZ, E., *Clay Minerals,* Akademiai Kiado, Budapest, Hungary, 1981, p. 119–123.

OLSSON, W. A. (1974), *Effects of temperature, pressure, and displacement rate on the frictional characteristics of a limestone.* Int. J. Rock Mech. Mining Sci. Geomech. Abstr. *11*, 267–278.

RIEDEL, W. (1929), *Zur mechanik geologischer Brucherscheinungen.* Zentralbl. Mineral Geol. Palaeont. *1929B*, 354–368.

SCHULTZ, L. G. (1964), 'Quantitative interpretation of mineralogical composition from X-rays and chemical data for the Pierre shale', in *Analytical Methods in Geochemical Investigation of the Pierre Shale.* U.S. Geol. Surv. Prof. Paper *391-C*, C1–C31.

SHIMAMOTO, T. (1977), *Effects of fault-gouge on the frictional properties of rocks: An experimental study.* Ph.D. Dissertation, Texas A and M Univ., p. 138–167.

SIBSON, R. H. (1982), *Fault zone models, heat flow, and the depth distribution of earthquakes in the continental crust of the United States.* Seism. Soc. Amer. Bull. *72*, 151–163.

SKEMPTON, A. W. (1966), *Some observations on tectonic shear zones.* Proc. 1st Congr. Internat. Soc. Rock Mech., Lisbon *1*, 329–335.

STESKY, R. M. (1978), *Rock friction—effect of confining pressure, temperature and pore pressure.* Pure Appl. Geophys. *116*, 690–704.

STESKY, R. M., BRACE, W. F., RILEY, D. K. and ROBIN, P.-Y. F. (1974), *Friction in faulted rock at high temperature and pressure.* Tectonophys. *23*, 177–203.

SUMMERS, R. and BYERLEE, J. (1977), *A note on the effect of fault gouge composition on the stability of frictional sliding.* Int. J. Rock Mech. Mining Sci. Geomech. Abstr. *14*, 155–160.

TCHALENKO, J. S. (1968), *The evolution of kink-bands and the development of compression textures in sheared clays.* Tectonophys. *6*, 159–174.

TCHALENKO, J. S. (1970), *Similarities between shear zones of different magnitudes.* Geol. Soc. Amer. Bull. *81*, 1625–1640.

TCHALENKO, J. S. and AMBRASEYS, N. N. (1970), *Structural analysis of the Dasht-e Baȳaz (Iran) earthquake fractures.* Geol. Soc. Amer. Bull. *81*, 41–60.

TEUFEL, L. W. and LOGAN, J. M. (1978), *Effect of displacement rate on the real area of contact and temperatures generated during frictional sliding of Tennessee sandstone.* Pure Appl. Geophys. *116*, 840–865.

WHITTAKER, E. J. W. and ZUSSMAN, J. (1956), *The characterization of serpentine minerals by X-ray diffraction.* Mineral Mag. *31*, 107–126.